Available online at www.sciencedirect.com

ScienceDirect

Energy Procedia 158 (2019) 4829–4833

Energy Procedia

www.elsevier.com/locate/procedia

10th International Conference on Applied Energy (ICAE2018), 22-25 August 2018, Hong Kong, China

Aluminum Storage in Rutile-based TiO_2 Nanoparticles

Tianyu Zhao[a], Manuel Ojeda[a], Jin Xuan[b], Zhan Shu[c], Huizhi Wang[d,*]

[a]*Research Centre for Carbon Solutions (RCCS), School of Engineering & Physical Sciences, Heriot-Watt University, Edinburgh, EH14 4AS, United Kingdom*

[b]*Department of Chemical Engineering, Loughborough University, Loughborough, LE11 3TU, United Kingdom*

[c]*Faculty of Engineering and the Envrionment, University of Southampton, Southampton, SO17 1BJ, United Kingdom*

[d]*Department of Mechanical Engineering, Imperial College London, Exhibition Road, South Kensington Campus, London, SW7 2AZ, United Kingdom*

Abstract

Aluminum storage in rutile-based TiO_2 nanoparticles was for the first time investigated. Electrochemical characteristics of rutile-based TiO_2 nanoparticles as an electrode for aluminum-ion batteries were studied using cyclic voltammetry, chronopotentiometry and electrochemical impedance spectroscopy. The first discharge capacity of 29.4 $mAh \cdot g^{-1}$ was achieved, and the value remains 22.6 $mAh \cdot g^{-1}$ after 50 cycles. The highest coulombic efficiency achieved at 89.8%.

Peer-review under responsibility of the scientific committee of ICAE2018 – The 10th International Conference on Applied Energy.

Keywords: TiO_2, Rechargeable batteries, Aluminium-ion batteries.

1. Introduction

To satisfy the rapidly increasing demand of the electronic storage devices in the market, rechargeable batteries have been treated as the most viable solution due to its high efficiency in many applications, such as electric vehicles and renewable energy industries.[1] Currently, Lithium-ion batteries (LIBs) is the most attractive commercial battery products in the market due to its high energy density feature and low self-discharge rate.[2] However, the high-cost, limited lithium resources and the safety concerns, as well as market demand necessitate the development of alternative storage solutions.

Numerous investigations on new rechargeable metal-ion batteries have been conducted.[3-6] Aluminum-ion batteries (AIBs) stand out not only due to the cost saving feature attributed to the aluminum abundance in the earth crust, the trivalent nature of aluminum offers more electrons to transfer and the lightweight feature also makes it a

* Corresponding author. Tel.: +44-207-594-7165.

Peer-review under responsibility of the scientific committee of ICAE2018 – The 10th International Conference on Applied Energy.
10.1016/j.egypro.2019.01.712

promising candidate to replace the LIBs.[7] The smaller radius of Al^{3+} (53.5 pm) is also beneficial for the ions to insert/extract into/from the host materials, which makes it the most attractive candidate.[6] Currently, most AIBs operate with non-aqueous electrolytes, which can be flammable, toxic and expensive. Therefore, using aqueous electrolytes can be more cost-effective and safer.[7]

TiO_2 materials have been widely applied in electrochemical studies due to its good chemical stability and non-toxicity feature. Different TiO_2 crystalline phases have been used as host materials for lithium storage.[8] Current research on AIBs has mainly focused on anatase materials. Recently a self-synthesized anatase TiO_2 as a working electrode for aluminum storage has shown promising results of 278 $mAh \cdot g^{-1}$ in aqueous AIBs.[9] However, there are limited works regarding other TiO_2 phases. As the most thermal stable phase, rutile TiO_2 as host electrode materials in LIBs has been widely reported and it worth studying in the AIBs.[2] Herein, we for the first time investigate the electrochemical aluminum storage into rutile TiO_2 for aluminum-ion batteries and study the mechanisms of the Al^{3+} storage.

2. Experimental

The electrochemical performance of rutile TiO_2 was studied in a three-electrode setup in an aqueous $AlCl_3$ electrolyte, using Pt wire and an Ag/AgCl (1 M KCl) electrode respectively as a counter electrode and a reference electrode. The TiO_2 electrode was prepared following the routine procedures.[9] Rutile TiO_2 (99.5 wt% trace metals based, Aldrich), Polyvinylidene difluoride (PVDF, Aldrich) and Acetylene carbon black (Strem Chemicals, INC.) were mixed with a weight ratio at 8:1:1, then dispersed in N-methylpyrrolidone (NMP, anhydrous 99.5 vol%, Sigma-Aldrich) to make an electrode ink. The mixture was treated in an ultrasonic bath (Fisher Bioblock Scientific) under 35 kHz for 1 h. Then, 5 μL of electrode ink was coated on a glassy carbon electrode (Jingke) with 2 mm diameter, dried at 50 °C in an oven for 2 h. 1M $AlCl_3$ solution was prepared from 6 N standard (2 M) $AlCl_3$ solution (Alfa Aesar) and 18.2 MΩ Milli-Q water (Millipore Corporation).

All electrochemical measurements were conducted at room temperature with a CHI 660C electrochemical workstation. Cyclic Voltammetry (CV) was performed between -0.4 to -1.3 V (vs. Ag/AgCl) at different scan rates from 1 $mV \cdot s^{-1}$ to 40 $mV \cdot s^{-1}$. The charge/discharge was performed with a potential window of -0.4 to -1.15 V (vs. Ag/AgCl). Electrochemical Impedance Spectroscopy (EIS) was performed at -1.1 V with a frequency range of 1 Hz to 1 MHz, with an amplitude of 5 mV.

3. Results and discussion

To study the reversible Al^{3+} storage in rutile TiO_2, CV was conducted and the results were shown in Figure 1. In Figure 1a, a clear pair of redox peaks can be observed at -1.09 and -0.80 V (vs. Ag/AgCl), respectively corresponding to Al^{3+} intercalation and extraction. An inconspicuous cathodic peak occurs at -0.81 V (vs. Ag/AgCl). A tiny anodic peak at -1.09 V (vs. Ag/AgCl) can be observed as well, which disappears in the following tests with increasing scan rates. At a scan rate of 1 $mV \cdot s^{-1}$ (Fig. 1a), the trend of hydrogen evolution reaction starts near -1.3 V (vs. Ag/AgCl) in the cathodic process. The peak positions indicate ensures the Al^{3+} insertion in preference to the hydrogen evolution by the strong solvation of aqueous ions, which contribute to high hydrogen evolution overpotential.[6]

To further evaluate the Al^{3+} insertion/extraction, CV at different scan rates was carried out and the results are shown in Figure 1b. The peak intensity of cathodic and anodic peak increases as the scan rate increases. At higher scan rate, the cathodic peak position moves more negative and closer to the hydrogen evolution potential. The inset shows the linear relationship between peak currents and the square root of the scan rate, which indicate that the solid phase diffusion reaction is dominant for Al^{3+} ions to insert into the rutile TiO_2 nanoparticles. It has been proposed in the literature that Al^{3+} storage in TiO_2 can follow the below reaction:[10]

$$xAl + TiO_2 \leftrightarrow Al_xTiO_2 \quad (1)$$

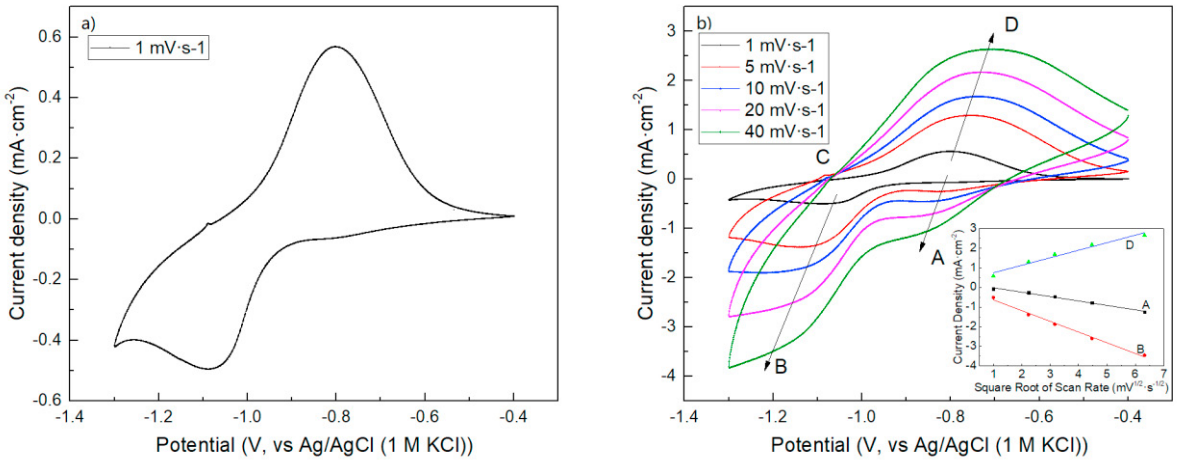

Figure 1. a) CV at 1 mV·s^{-1}; b) CV with different scan rates. The inset in b) is the relationship between the cathodic peak current densities and scan rates, symbols are experimental data and lines are fitted data.

To demonstrate Al^{3+} insertion into rutile TiO_2 electrode, the typical charge/discharge curves and electrochemical cycling performance are shown in Figure 2. A flat charge plateau at around -1.05 V (vs. Ag/AgCl) can be observed in Figure 2a, which is slightly higher than the insertion peak position from CV results. However, unlike the study of anatase materials, a clear discharge plateau appears around -0.95 V (vs. Ag/AgCl), which is lower than the potential result from CVs.[6] In Figure 2b, The discharge capacity at the 1st cycle is 29.4 mAh·g^{-1} and continuously decreases to 22.6 mAh·g^{-1} after 50 cycles, which is 76.7% of the initial discharge capacity. It drops quickly in the first 10 cycles than the following cycles. On the other hand, the initial charge capacity is 38.7 mAh·g^{-1}, and it drops rapidly to 32.3 mAh·g^{-1} in the 2nd cycle. Unlike to discharge profiles, the charge capacity increases after 30 cycles and this phenomenon may result by electrode coating degradation, which also leads to the reduction of coulombic efficiency. The highest coulombic efficiency reached 89.8% at the 7th cycle.

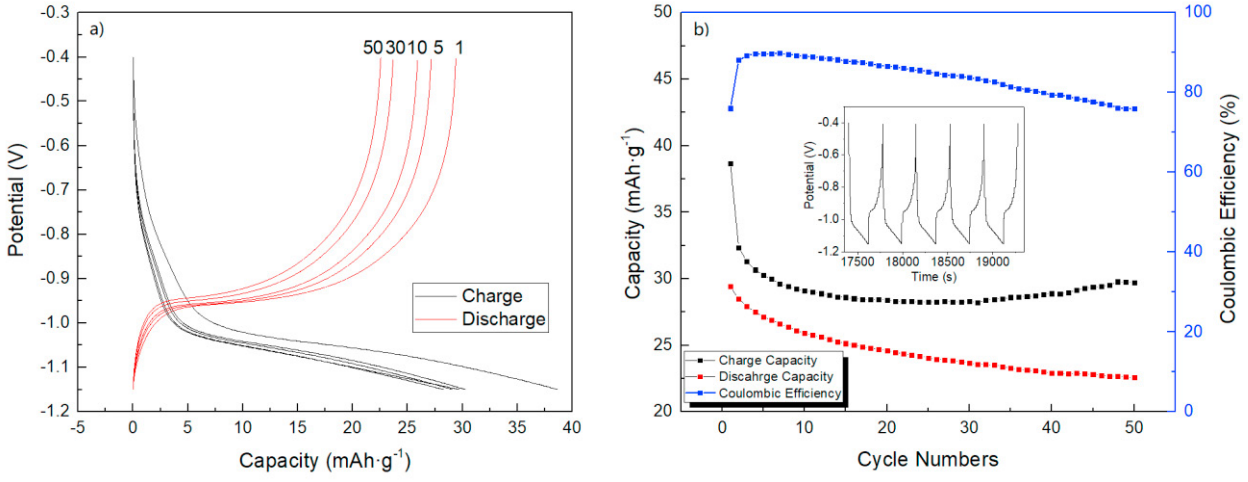

Figure 2. a) Charge/discharge curves at different cycles; b) Cycling performance in 50 cycles at 0.5 A·g^{-1}. The inset is the last 5 cycles.

To better explain the degradation against cycle number, EIS measurement at different cycles was carried out and the results are shown in Figure 3a. The depressed semicircles can be observed at a high-frequency region in the Nyquist

plots corresponding to charge transfer process. Meanwhile, the linear plot at low-frequency range reflects the Al^{3+} diffusion impedance inside the electrode, also known as Warburg impedance, indicates the diffusion steps mainly controlled the electrode process both before and after the electrode being cycled. The appeared semicircles represent the charge-transfer process, while the increasing linear plot at low-frequency range represents the Warburg impedance which is attributed to the Al^{3+} diffusion in the electrode. An equivalent circuit model was constructed and showed in the insert figure of Figure 3.[9] The resistance R_e represents the resistance of the electrolyte. In the first parallel circuit branch, the capacitance C_{SEI} and resistance R_{SEI} represents the capacitance and resistance of the interfacial film between the particles and the current collector, respectively. In the second branch, the capacitance R_{ct} is the charge transfer resistance which reflecting the Al^{3+} insertion/extraction into/from the TiO_2, and the capacitance C_{ic} represents to the interfacial capacitance between electrode and electrolyte. Table 1 presents the values of all the components. From Table 1, the electrolyte resistance R_e slightly decreases while the cycle number is increasing. And the charge transfer resistance keeps around 24.5 Ω. The slope of the low-frequency region represents the Warburg coefficient, and the decreases value indicates lower Warburg impedance.

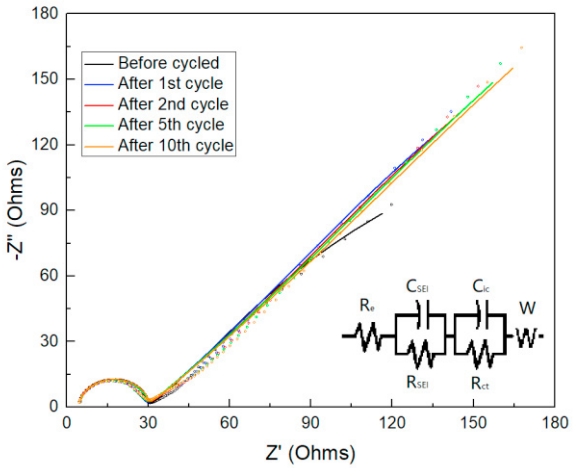

Figure 3. EIS Nyquist plots. Symbols are experimental data and lines are fitted data. The inset is the corresponding equivalent circuit.

Table 1. Impedance parameters.

Cycles	R_e (Ω)	C_{SEI} (*F*)	R_{SEI} (Ω)	C_{ic} (*F*)	R_{ct} (Ω)	W (Ω)
After 1st cycle	4.690	4.790E-003	88.45	6.272E-008	24.37	2.839E-003
After 2nd cycle	4.612	5.004E-003	98.19	6.485E-008	24.58	2.554E-003
After 5th cycle	4.547	5.175E-003	108.3	6.807E-008	24.39	2.352E-003
After 10th cycle	4.489	5.515E-003	108.4	6.877E-008	24.68	2.203E-003

4. Conclusion

The aluminum storage behavior in rutile TiO_2 nanoparticles in a 1 M $AlCl_3$ aqueous electrolyte was investigated. The aluminum insertion process is mainly controlled by solid phase diffusion reaction. The initial discharge capacity is 29.4 mAh·g^{-1}, which remains 22.6 mAh·g^{-1} after 50 cycles, with the highest coulombic efficiency of 89.8%. EIS measurements show that the impedance increases gradually with the cycle number, different from the anatase TiO_2 where the impedance at the 1st cycle is higher than the following cycles. This work may contribute to developing new TiO_2 host materials for the aqueous AIBs.

Acknowledgement

The authors acknowledge support from the Engineering and Physical Sciences Research Council (EPSRC) under grants EP/S000933/1 and EP/N009924/1. The research is also supported by the European Union's Horizon 2020 research and innovation Programme under grant agreement No. 734796.

Reference

[1] Klavetter KC, Pedro de Souza J, Heller A, Mullins CB. High tap density microparticles of selenium-doped germanium as a high efficiency, stable cycling lithium-ion battery anode material. Journal of Materials Chemistry A. 2015;3(11):5829-34.
[2] Ge H, Hao T, Zhang B, Chen L, Cui L, Song X-M. Nanoparticles-Constructed Spinel $Li_4Ti_5O_{12}$ with Extra Surface Lithium Storage Capability towards Advanced Lithium-ion Batteries. Electrochimica Acta. 2016;211:119-25.
[3] Palomares V, Serras P, Villaluenga I, Hueso KB, Carretero-González J, Rojo T. Na-ion batteries, recent advances and present challenges to become low cost energy storage systems. Energy & Environmental Science. 2012;5(3):5884.
[4] Tao ZL, Xu LN, Gou XL, Chen J, Yuan HT. TiS_2 nanotubes as the cathode materials of Mg-ion batteries. Chem Commun (Camb). 2004(18):2080-1.
[5] Xu C, Li B, Du H, Kang F. Energetic zinc ion chemistry: the rechargeable zinc ion battery. Angew Chem Int Ed Engl. 2012;51(4):933-5.
[6] Liu S, Hu JJ, Yan NF, Pan GL, Li GR, Gao XP. Aluminum storage behavior of anatase TiO_2 nanotube arrays in aqueous solution for aluminum ion batteries. Energy & Environmental Science. 2012;5(12):9743.
[7] Antonio EG, Krystan M, Katrin H, Sebastien F, Rongying L, Etienne K, et al. An Overview and Future Perspectives of Aluminum Batteries. Advanced Materials. 2016;28(35):7564-79.
[8] Aravindan V, Lee Y-S, Yazami R, Madhavi S. TiO_2 polymorphs in 'rocking-chair' Li-ion batteries. Materials Today. 2015;18(6):345-51.
[9] He YJ, Peng JF, Chu W, Li YZ, Tong DG. Black mesoporous anatase TiO_2 nanoleaves: a high capacity and high rate anode for aqueous Al-ion batteries. J Mater Chem A. 2014;2(6):1721-31.
[10] Tang W, Xuan J, Wang H, Zhao S, Liu H. First-principles investigation of aluminum intercalation and diffusion in TiO_2 materials: Anatase versus rutile. Journal of Power Sources. 2018;384:249-55.